

## Nickel(II)–Phenoxy Radical Complexes: Structure–Radical Stability Relationship

Yuichi Shimazaki,<sup>\*,†</sup> Stefan Huth,<sup>‡,§</sup> Satoru Karasawa,<sup>||</sup> Shun Hirota,<sup>‡,⊥</sup> Yoshinori Naruta,<sup>†</sup> and Osamu Yamauchi<sup>\*,#</sup>

Institute for Materials Chemistry and Engineering, Kyushu University, Higashi-ku, Fukuoka 812-8581, Japan, Department of Chemistry, Graduate School of Science, Nagoya University, Chikusa-ku, Nagoya 464-8602, Japan, Graduate School of Pharmaceutical Sciences, Kyushu University, Higashi-ku, Fukuoka 812-8582, Japan, and Unit of Chemistry, Faculty of Engineering, Kansai University, Suita, Osaka 564-8680, Japan

Received July 20, 2004

Nickel(II) complexes of N<sub>3</sub>O-donor tripodal ligands, 2,4-di-*tert*-butyl-6-{([bis(2-pyridyl)methyl]amino)methyl}phenol (HtbuL), 2,4-di-*tert*-butyl-6-{([(6-methyl-2-pyridyl)methyl](2-pyridylmethyl)amino)methyl}phenol (HtbuLMepy), and 2,4-di-*tert*-butyl-6-{([bis(6-methyl-2-pyridyl)methyl]amino)methyl}phenol (HtbuL(Mepy)<sub>2</sub>), were prepared, and [Ni(tbuL)Cl(H<sub>2</sub>O)] (**1**), [Ni(tbuLMepy)Cl] (**2**), and [Ni(tbuL(Mepy)<sub>2</sub>)Cl] (**3**) were structurally characterized by the X-ray diffraction method. Complexes **1** and **3** have a mononuclear structure with a coordinated phenolate moiety, while **2** has a dinuclear structure bridged by two chloride ions. The geometry of the Ni(II) center was found to be octahedral for **1** and **2** and 5-coordinate trigonal bipyramidal for **3**. Complexes **1**–**3** exhibited similar absorption spectra in CH<sub>3</sub>CN, indicating that they all have a mononuclear structure in solution. They were converted to the phenoxy radicals upon oxidation with Ce(IV), giving a phenoxy radical  $\pi$ – $\pi^*$  transition band at 394–407 nm. ESR spectra at low temperature and resonance Raman spectra established that the radical species has a Ni(II)–phenoxy radical bond. The cyclic voltammograms showed a quasi-reversible redox wave at  $E_{1/2} = 0.46$ – $0.56$  V (vs Ag/AgCl) corresponding to the formation of the phenoxy radical, which displayed a first-order decay with a half-life of 45 min at room temperature for **1** and 26 and 5.9 min at  $-20$  °C for **2** and **3**, respectively. The radical stability increased with the donor ability of the N ligands.

## Introduction

The coordination chemistry of the phenoxy radical has been intensively studied in recent years due to its occurrence in the active site of galactose oxidase (GOase), which contains one copper ion and performs the oxidation of a primary alcohol to the aldehyde in the presence of dioxygen.<sup>1–5</sup> We reported earlier the formation and stability of the

phenoxy radical species by one-electron oxidation of the Cu(II) and Zn(II) complexes of tripodal N<sub>3</sub>O ligands derived from N-functionalized 2-pyridylmethylamine with a pendent

\* Authors to whom correspondence should be addressed. E-mail: yshima@ms.ifoc.kyushu.ac.jp (Y.S.), osamuy@ipcku.kansai-u.ac.jp (O.Y.). Fax: +81-6-6330-3770 (O.Y.).

<sup>†</sup> Institute for Materials Chemistry and Engineering, Kyushu University.

<sup>‡</sup> Nagoya University.

<sup>§</sup> On leave of absence from the University of Bremen.

<sup>||</sup> Faculty of Pharmaceutical Sciences, Kyushu University.

<sup>⊥</sup> Present address: Kyoto Pharmaceutical University, Yamashina-ku, Kyoto 607-8413, Japan.

<sup>#</sup> Kansai University.

(1) (a) Whittaker, J. W. *Met. Ions Biol. Syst.* **1994**, *30*, 315. (b) Whittaker, J. W. In *Bioinorganic Chemistry of Copper*; Karlin, K. D., Tyeklar, Z., Eds.; Chapman & Hall: New York, 1993; p 447.

- (2) (a) Itoh, N.; Phillips, S. E. V.; Stevens, C.; Ogel, Z. B.; McPherson, M. J.; Keen, J. N.; Yadav, K. D. S.; Knowles, P. F. *Nature* **1991**, *350*, 87. (b) Itoh, N.; Phillips, S. E. V.; Stevens, C.; Ogel, Z. B.; McPherson, M. J.; Keen, J. N.; Yadav, K. D. S.; Knowles, P. F. *Faraday Discuss.* **1992**, *93*, 75. (c) Itoh, N.; Phillips, S. E. V.; Yadav, K. D. S.; Knowles, P. F. *J. Biol. Chem.* **1994**, *238*, 794.
- (3) (a) Whittaker, M. M.; Whittaker, J. W.; Milburn, H.; Quick, A. J. *J. Biol. Chem.* **1990**, *265*, 9610. (b) McGlashen, M. L.; Eads, D. D.; Spiro, T. G.; Whittaker, J. W. *J. Phys. Chem.* **1995**, *99*, 4918. (c) Baron, A. J.; Stevens, C.; Wilmot, C.; Seneviratne, K. D.; Blakeley, V.; Dooley, D. M.; Phillips, S. E. V.; Knowles, P. F.; McPherson, M. J. *J. Biol. Chem.* **1994**, *269*, 25095. (d) Knowles, P. F.; Brown III, R. D.; Koenig, S. H.; Wang, S.; Scott, R. A.; McGuire, M. A.; Brown, D. E.; Dooley, D. M.; *Inorg. Chem.* **1995**, *34*, 3895. (e) Reynolds, M. P.; Baron, A. J.; Wilmot, C. M.; Vinecombe, E.; Steven, C.; Phillips, S. E. V.; Knowles, P. F.; MacPerson, M. J. *J. Biol. Inorg. Chem.* **1997**, *2*, 327.
- (4) Stubbe, J.; van der Donk, W. A. *Chem. Rev.* **1998**, *98*, 705.
- (5) Chaudhuri, P.; Wieghardt, K. *Prog. Inorg. Chem.* **2001**, *50*, 151–216.

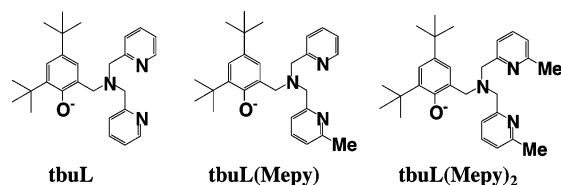


Figure 1. Structures of ligands.

phenolate moiety with bulky substituents.<sup>6</sup> The stability of the Cu(II)–phenoxy radical from the complexes depended upon the donor properties of equatorial nitrogen atoms; with weaker equatorial nitrogen donors, the phenoxy radical was less stable and the potential of the phenoxy radical formation was higher. The reaction of Cu(ClO<sub>4</sub>)<sub>2</sub>·6H<sub>2</sub>O with the N<sub>2</sub>O<sub>2</sub>-donor ligands containing a phenol moiety with two bulky substituents gave the Cu(II)–phenoxy radical species by disproportionation,<sup>7</sup> and we could isolate a Cu(II)–phenoxy radical complex having an *o*-methoxyphenol moiety by disproportionation. These results suggest that the formation and stability of Cu(II)–phenoxy radical species depend on the ligand field effect.<sup>8</sup>

On the other hand, only two types of Ni(II)–phenoxy radical species have been reported.<sup>9,10</sup> We have reported that oxidation of a low-spin d<sup>8</sup> Ni(II)–salen complex having salicylidene moieties with two bulky substituents led to a temperature-dependent tautomerism between the Ni(II)–phenoxy radical and Ni(III)–phenolate states with the same *S* = 1/2 spin state.<sup>9</sup> In contrast, oxidation of the high-spin d<sup>8</sup> Ni(II) complexes of 1,4,7-triazacyclononane macrocyclic ligands with a pendent phenol ring yielded Ni(II)–phenoxy radical species, which had an *S* = 3/2 ground state with the ferromagnetically coupled Ni(II) and phenoxy radical electrons.<sup>10</sup> The properties of Ni(II)–phenoxy radical complexes are therefore expected to be dependent on factors such as the ligand field and temperature.

We now studied synthesis of the Ni(II)–phenolate complexes of a series of N<sub>3</sub>O-donor tripodal ligands containing a phenolate moiety with bulky substituents (Figure 1), chemical and electrochemical generation of the one-electron oxidized phenoxy radical species in CH<sub>3</sub>CN, and characterization of their electronic structure by absorption, ESR, and resonance Raman spectroscopies. We further investigated the influence of the ligand donor ability on the nickel site structure and formation and stability of the phenoxy radical species.

## Experimental Section

**Materials and Methods.** All the chemicals used were of the highest grade available and were further purified whenever neces-

sary.<sup>11</sup> Solvents were also purified before use by standard methods.<sup>11</sup> The synthesis of ligands, HtbuL, HtbuLMepy, and HtbuL(Mepy)<sub>2</sub> (Figure 1), has been reported previously.<sup>6</sup> Electronic spectra were obtained with a Shimadzu UV-3101PC spectrophotometer. Electrochemical measurements were carried out in a conventional three-electrode cell for samples (1 mM) dissolved in dry CH<sub>3</sub>CN containing 0.1 M tetra-*n*-butylammonium perchlorate (TBAP). A glassy-carbon electrode and a platinum wire were used as a working and a counter electrode, respectively, with an Ag/AgCl reference electrode used in all the experiments. The reversibility of the electrochemical processes was evaluated by standard procedures and referenced against the ferrocene/ferrocenium redox couple. Frozen-solution ESR spectra were acquired by a JEOL JES-RE1X X-band spectrometer equipped with a standard low-temperature apparatus. The spectra were recorded at 77 K by using quartz tubes with a 4-mm inner diameter. Microwave frequency was standardized against a Mn(II) marker. Resonance Raman spectra were measured with a JASCO NR-1800 triple polychromator equipped with a liquid-nitrogen-cooled Princeton Instruments CCD detector. Raman shifts were calibrated with acetone, the accuracy of the peak positions of the Raman bands being ±1 cm<sup>-1</sup>. Variable-temperature magnetic susceptibility data were measured for a polycrystalline sample of complex **2** with a HOXSAN HSM-D SQUID susceptometer in the temperature range 5–300 K with an applied field of 5000 G. A diamagnetic correction, estimated from Pascal's constants, was subtracted from the experimental susceptibilities to give the molecular paramagnetic susceptibilities.

**Synthesis of Complexes. [Ni(tbuL)Cl(H<sub>2</sub>O)] (1).** To a solution of HtbuL (0.417 g, 1.0 mmol) in methanol (10 mL) was added NiCl<sub>2</sub>·6H<sub>2</sub>O (0.238 g, 1.0 mmol), and the resulting solution was mixed with a few drops of triethylamine and left to stand for a few days at room temperature. The pale blue microcrystals obtained were recrystallized from CH<sub>3</sub>CN. Yield: 0.266 g (50%). Anal. Found: C, 61.46; H, 6.899; N, 8.039. Calcd for C<sub>27</sub>H<sub>38</sub>N<sub>3</sub>O<sub>2</sub>ClNi: C, 61.33; H, 6.68; N, 7.95.

**[Ni(tbuLMepy)Cl] (2).** This complex was prepared in a similar manner in 74% yield. Anal. Found: C, 64.03; H, 6.993; N, 8.018. Calcd for C<sub>28</sub>H<sub>38</sub>N<sub>3</sub>OCINi: C, 64.09; H, 6.91; N, 8.01.

**[Ni(tbuL(Mepy)<sub>2</sub>)Cl] (3).** This complex was prepared in a similar manner in 76% yield. Anal. Found: C, 64.59; H, 7.148; N, 7.761. Calcd for C<sub>29</sub>H<sub>40</sub>N<sub>3</sub>OCINi: C, 64.65; H, 7.11; N, 7.80.

**X-ray Structure Determination.** The X-ray experiments were carried out for the well-shaped single crystals of complexes **1–3** on a Rigaku RAXIS imaging plate area detector with graphite-monochromated Mo K $\alpha$  radiation ( $\lambda$  = 0.710 73 Å). The crystals were mounted on a glass fiber. To determine the cell constants and orientation matrix, three oscillation photographs were taken for each frame with the oscillation angle of 3° and the exposure time of 3 min. Reflection data were corrected for both Lorentz and polarization effects. The structures were solved by the heavy-atom method and refined anisotropically for non-hydrogen atoms by full-matrix least-squares calculations. Each refinement was continued until all shifts were smaller than one-third of the standard deviations of the parameters involved. Atomic scattering factors and anomalous dispersion terms were taken from the literature.<sup>12</sup> Hydrogen atoms except for the water were located at the calculated positions and were assigned a fixed displacement and constrained to ideal geometry with C–H = 0.95 Å. The thermal parameters of calculated hydrogen atoms were related to those of their parent atoms

(6) Shimazaki, Y.; Huth, S.; Hirota, S.; Yamauchi, O. *Bull. Chem. Soc. Jpn.* **2000**, *73*, 1187.

(7) Shimazaki, Y.; Huth, S.; Odani, A.; Yamauchi, O. *Angew. Chem., Int. Ed.* **2000**, *39*, 1666.

(8) Shimazaki, Y.; Huth, S.; Hirota, S.; Yamauchi, O. *Inorg. Chim. Acta* **2002**, *331*, 168.

(9) Shimazaki, Y.; Tani, F.; Fukui, K.; Naruta, Y.; Yamauchi, O. *J. Am. Chem. Soc.* **2003**, *125*, 10513.

(10) Müller, J.; Kikuchi, A.; Bill, E.; Weyhermüller, T.; Hildebrandt, P.; Ould-Moussa, L.; Wieghardt, K. *Inorg. Chim. Acta* **2000**, *297*, 265.

(11) Perrin, D. D.; Armarego, W. L. F.; Perrin, D. R. *Purification of Laboratory Chemicals*; Pergamon Press: Elmsford, NY, 1966.

(12) Ibers, J. A.; Hamilton, W. C., Eds. *International Tables for X-ray Crystallography*; Kynoch: Birmingham, U.K., 1974; Vol. IV.

**Table 1.** Crystal Data for Ni(II) Complexes 1–3

	1	2	3
formula	C <sub>27</sub> H <sub>36</sub> N <sub>3</sub> O <sub>2</sub> NiCl	C <sub>28</sub> H <sub>36</sub> N <sub>3</sub> ONiCl	C <sub>29</sub> H <sub>38</sub> N <sub>3</sub> ONiCl
fw	528.75	524.76	538.79
color	pale blue	green	brown
cryst size/mm	0.11 × 0.27 × 0.07	0.15 × 0.10 × 0.07	0.11 × 0.10 × 0.05
cryst system	monoclinic	monoclinic	orthorhombic
space group	<i>P2<sub>1</sub>/c</i>	<i>P2<sub>1</sub>/a</i>	<i>Pbca</i>
<i>a</i> (Å)	14.8708(7)	10.475(4)	10.7377(3)
<i>b</i> (Å)	9.9638(4)	18.482(6)	15.1861(3)
<i>c</i> (Å)	17.9492(9)	13.785(6)	35.4669(9)
$\beta$ (deg)	92.2701(8)	100.06(1)	
<i>V</i> (Å <sup>3</sup> )	2657.4(2)	2627(1)	5783.3(3)
<i>Z</i>	4	4	8
$\mu$ (Mo K $\alpha$ ) (cm <sup>-1</sup> )	8.59	8.65	7.88
<i>F</i> (000)	1120.00	1112.00	2288.00
$2\theta_{\max}$ (deg)	55.0	55.0	54.9
no. of reflns obsd	24 266	25 204	35 419
no. of reflns used	6042	6005	6558
no. of variables	307	307	316
<i>R</i> [ <i>I</i> = 2 $\sigma$ ( <i>I</i> )]	0.061	0.051	0.059
<i>R<sub>w</sub></i>	0.140	0.064	0.151

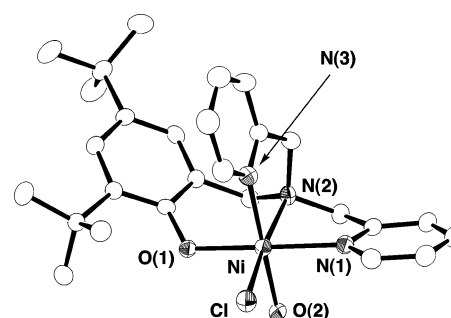
**Table 2.** Selected Bond Distances (Å) and Angles (deg) of Complexes 1–3

	1	2	3
Distances			
Ni(1)–Cl(1)	2.406(1)	2.4118(8)	2.295(2)
Ni(1)–Cl(1)*		2.479(1)	
Ni(1)–O(1)	2.066(3)	2.017(2)	1.954(4)
Ni(1)–O(2)	2.061(3)		
Ni(1)–N(1)	2.106(4)	2.143(3)	2.125(4)
Ni(1)–N(2)	2.119(4)	2.091(2)	2.046(5)
Ni(1)–N(3)	2.070(4)	2.096(3)	2.134(5)
Angles			
Cl(1)–Ni(1)–Cl(1)*		83.65(3)	
Cl(1)–Ni(1)–O(1)	96.70(9)	92.67(6)	140.1(1)
Cl(1)–Ni(1)–O(2)	92.89(9)		
Cl(1)–Ni(1)–N(1)	93.8(1)	106.06(7)	91.0(1)
Cl(1)–Ni(1)–N(2)	171.2(1)	172.34(7)	123.5(1)
Cl(1)–Ni(1)–N(3)	95.4(1)	93.35(8)	95.2(1)
Cl(1)*–Ni(1)–O(1)		176.17(6)	
Cl(1)*–Ni(1)–N(1)		89.62(6)	
Cl(1)*–Ni(1)–N(2)		91.25(7)	
Cl(1)*–Ni(1)–N(3)		88.80(7)	
O(1)–Ni(1)–O(2)	86.5(1)		
O(1)–Ni(1)–N(1)	167.7(1)	90.41(8)	93.8(2)
O(1)–Ni(1)–N(2)	91.4(1)	92.52(9)	96.3(2)
O(1)–Ni(1)–N(3)	90.6(1)	92.46(9)	92.8(2)
O(2)–Ni(1)–N(1)	86.7(1)		
O(2)–Ni(1)–N(2)	91.1(1)		
O(2)–Ni(1)–N(3)	171.5(1)		
N(1)–Ni(1)–N(2)	78.6(1)	79.54(10)	79.2(2)
N(1)–Ni(1)–N(3)	94.7(2)	160.22(10)	161.1(2)
N(2)–Ni(1)–N(3)	81.0(1)	80.79(10)	82.5(2)

by  $U(H) = 1.2U_{eq}(C)$ . The hydrogen atoms of the water molecule of **1** were located from the difference Fourier maps. All the calculations were performed by using the TEXSAN program package.<sup>13</sup> Summaries of the fundamental crystal data and experimental parameters for structure determination are given in Table 1.

## Results and Discussion

**Crystal Structures of Ni(II)–Phenolate Complexes.** The ORTEP views of complexes **1**–**3** are shown in Figures 2–4, respectively, and the selected bond lengths and angles are listed in Table 2. All the complexes were phenolate

**Figure 2.** ORTEP view of [Ni(tbuL)Cl(H<sub>2</sub>O)] (**1**) drawn with the thermal ellipsoids at the 50% probability level and atomic labeling scheme.

complexes with one chloride ion coordinated to the Ni center. The structure of **1** has an octahedral geometry formed by a phenolate oxygen, two pyridine nitrogens, a tertiary nitrogen, a chloride ion, and a water oxygen (Figure 2). Three nitrogen atoms of **1** assume a *fac*-configuration with the Ni–O(phenolate) and Ni–N bond distances, Ni–O(1) = 2.066(3), Ni–N(1) = 2.106(4), Ni–N(2) = 2.119(4), and Ni–N(3) = 2.070(4) Å, the Ni–N(2)(tertiary nitrogen) bond distance being slightly longer than the Ni–pyridine nitrogen distances. Complex **2** has a dinuclear structure bridged by two chloride ions, where each nickel site has an octahedral geometry formed by a phenolate oxygen, two pyridine nitrogens, a tertiary nitrogen, and two bridged chloride ions (Figure 3). Three nitrogen atoms of **2** assume a *mer*-configuration with the Ni–N bond distances, Ni–N(1) = 2.143(4), Ni–N(2) = 2.091(4), and Ni–N(3) = 2.096(4) Å, and the Ni–O(1) distance, 2.017(2) Å. Complex **2** differs from the Cu(II) complex of the same ligand, which has a square-pyramidal structure with the 2-methylpyridine nitrogen at an apical position.<sup>6</sup> The Ni–O(phenolate) bond length in **2** (2.017(2) Å) is slightly shorter than that of **1**, but the Ni–N(2-methylpyridine) distance (2.143(4) Å) is longer than that of **1**, probably due to the steric hindrance of the methyl group of 2-methylpyridine moiety in **2**. The structure of **3** (Figure 4) differs significantly from that of **1** and **2** as it has a distorted trigonal-bipyramidal geometry formed by a phenolate oxygen, two 2-methylpyridine nitrogens, a tertiary nitrogen, and a chloride ion with the distances, Ni–O(1) =

(13) *Crystal Structure Analysis Package*; Molecular Structure Corp.: The Woodlands, TX, 1985, 1999.

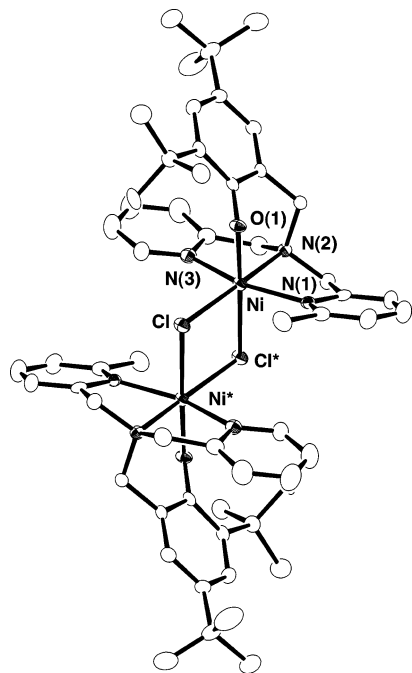


**Figure 3.** ORTEP view of [Ni(tbuLMepy)Cl] (**2**) drawn with the thermal ellipsoids at the 50% probability level and atomic labeling scheme.

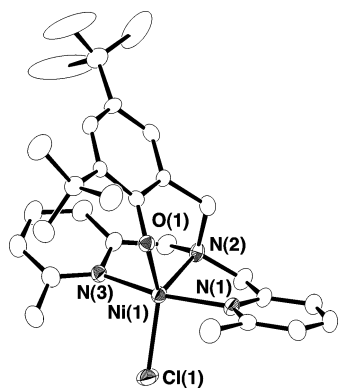


**Figure 4.** ORTEP view of [Ni(tbuL(Mepy)<sub>2</sub>)Cl] (**3**) drawn with the thermal ellipsoids at the 50% probability level and atomic labeling scheme.

1.954(4), Ni–N(1) = 2.125(4), Ni–N(2) = 2.046(5), and Ni–N(3) = 2.134(5) Å, respectively. The relative extent of the trigonal-bipyramidal distortion is indicated by an index  $\tau$  representing the degree of trigonality within the structural continuum between square-planar and trigonal-bipyramidal structures.<sup>14</sup> The  $\tau$  value of the Ni center of **3** is calculated to be 0.35 according to the equation  $\tau = (\beta - \alpha)/60$ , where  $\alpha = \text{Cl}(1)\text{--Ni}(1)\text{--O}(1)$  ( $140.1(1)^\circ$ ) and  $\beta = \text{N}(1)\text{--Ni}(1)\text{--N}(3)$  ( $161.1(2)^\circ$ ). As  $\tau$  is 0 and 1 for a perfect square-planar and a perfect trigonal geometry, respectively, the structure of **3** may be described as distorted square-planar geometry. The two 2-methylpyridine nitrogens are bound at axial positions, since the donor ability of 2-methylpyridine moiety is lower than that of unsubstituted pyridine donor.<sup>15</sup> In this connection, the Ni–O(phenolate) bond length increased in the order **3** (1.953(3) Å) < **2** (2.017(5) Å) < **1** (2.054(4)

(14) Addison, A. W.; Rao, T. N.; Reedijk, J.; von Rijn, J.; Verschoor, G. C. *J. Chem. Soc., Dalton Trans.*, **1984**, 1349.

(15) Nagao, H.; Komeda, N.; Mukaida, M.; Suzuki, M.; Tanaka, K. *Inorg. Chem.* **1996**, *35*, 6809.

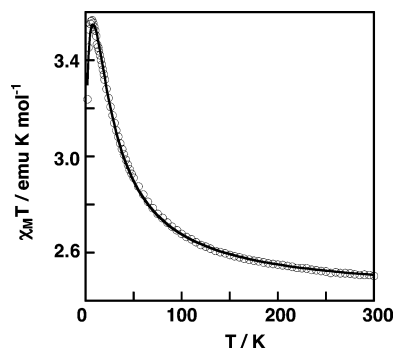


**Figure 5.** Thermal dependence of the  $\chi_M T$  for **2**. The solid line represents the fitted curve.

Å). This tendency has been observed for the Cu(II) complexes of the same ligand series.<sup>5</sup> However, the geometry of the Cu(II) complex corresponding to **3** has a square-pyramidal structure with equatorial phenolate coordination, which is different from the geometry of **3**.

**Magnetic Susceptibilities of Ni(II)–Phenolate Complexes.** The Ni(II) complexes **1–3** were paramagnetic  $d^8$  high-spin Ni(II) species, since the effective magnetic moment ( $\mu_{\text{eff}}$ ) of the monomeric complexes **1** and **3** at 287 K is 3.01 and 3.16  $\mu_B$  (1.13 and 1.25 emu K mol<sup>-1</sup>), respectively, and no sharp <sup>1</sup>H NMR spectra were observed in the diamagnetic region. Figure 5 shows the temperature dependence of the observed magnetic susceptibility,  $\chi_M$ , of the dinuclear complex **2**, whose observed  $\chi_M T$  value of 2.60 emu K mol<sup>-1</sup> at 300 K is in good agreement with the values of two isolated nickel spin center calculated for  $S = 1$  and  $g = 2.28$ . A gradual increase in the  $\chi_M T$  value was observed as the temperature was decreased from 300 to 7 K, indicating the presence of a ferromagnetic interaction within a molecule. The value reached its maximum of 3.54 emu K mol<sup>-1</sup> at 7 K, which is closer to the theoretical value for  $S_T = 2$  resulting from the ferromagnetic coupling of two  $S_{\text{Ni}} = 1$  centers through the bridged chloride ions. The experimental data for **2** was fitted by using eq 1, which was derived from the isotropic spin Hamiltonian  $H = -2JS_1 \cdot S_2$ :<sup>16</sup>

$$\chi_M = \frac{Ng^2\beta^2}{3k(T - \Theta)} \left[ \frac{30 \exp(6J/kT) + 6 \exp(2J/kT)}{5 \exp(6J/kT) + 3 \exp(2J/kT) + 1} \right] + N\alpha \quad (1)$$

Here  $J$  is the intradimer exchange interaction,  $\Theta$  is the interdimer exchange interaction, and  $N\alpha$  is the term of the temperature-independent paramagnetism (TIP). The parameters for the best fit were  $g = 2.25$ ,  $2J = 5.35$  cm<sup>-1</sup>, and  $\Theta = -0.49$  cm<sup>-1</sup>, respectively, and the theoretical curve is represented by a solid line in Figure 5. Detailed analysis of the magnetic properties of dinuclear Ni(II) complexes normally requires the calculation by the Ginsberg equation, which takes into account the axial anisotropy and zero-field splitting effects.<sup>17</sup> However, these parameters were not explicitly considered in the present calculation, since the

(16) O'Connor, C. J. *Prog. Inorg. Chem.* **1982**, *29*, 203.

(17) Ginsberg, A. P.; Martin, R. L.; Brookes, R. W.; Sherwood, R. C. *Inorg. Chem.* **1972**, *11*, 2884.

**Table 3.** Properties of the Ni(II), Cu(II), and Zn(II) Complexes and Their Phenoxy Radical Species

complex	$\lambda_{\max}/\text{nm}^a$ ( $\epsilon/\text{M}^{-1}\text{cm}^{-1}$ )	redox potential ( $E_{1/2}/\text{V}$ ) of phenolate/phenoxy	decay const/ $\text{s}^{-1}$ (half-life/min, temp/ $^{\circ}\text{C}$ )	ref
[Ni(tbuL)Cl(H <sub>2</sub> O)] (1)	405 (2500), 457 (1100), 495 (1200), 660 (500), 1120 (400)	0.46	$2.48 \times 10^{-4}$ (45, 20)	this work
[Ni(tbuLMepy)Cl] (2)	407 (2000), 462 (1000), 734 (350), 1110 (100)	0.49	$4.38 \times 10^{-4}$ (26, -20)	this work
[Ni(tbuL(Mepy) <sub>2</sub> )Cl] (3)	394 (2000), 479 (1000), 739 (350), 1140 (100)	0.56	$1.95 \times 10^{-3}$ (5.9, -20)	this work
[Ni(tbu-salcn)]	311 (9100), 374 (7200), 430 (3500), 881 (1000), 1103 (3000)	0.88, 1.22	not determined	9
[Cu(HtbuL)Cl]ClO <sub>4</sub>	not determined	1.17	not determined	6
[Cu(tbuLMepy)Cl]	418 (3500), 666 (420)	0.56	$1.86 \times 10^{-4}$ (65, -20)	6
[Cu(tbuL(Mepy) <sub>2</sub> )Cl]	406 (2000), 664 (410)	0.61	$1.28 \times 10^{-3}$ (9.0, -40)	6
[Zn(tbuL)Cl]	405 (3200), 678 (400)	0.69	$1.31 \times 10^{-4}$ (88, -20)	6
Cu(ClO <sub>4</sub> ) <sub>2</sub> ·6H <sub>2</sub> O + H <sub>2</sub> L <sup>b</sup>	410 (4000), 422 (3800), 672 (1000)	not determined	$9.3 \times 10^{-4}$ (12.4, -20)	7
[Cu(MeOL2)] <sub>2</sub> (ClO <sub>4</sub> ) <sub>2</sub> <sup>c</sup>	478 (4500)	0.35	$3.70 \times 10^{-5}$ (315, 20)	8

<sup>a</sup> Values for the radical species. <sup>b</sup> H<sub>2</sub>L = *N*-(2-pyridylmethyl)-*N,N*-bis(2'-hydroxy-3',5'-di-*tert*-butylbenzyl)amine. <sup>c</sup> MeOL2 = *N*-(1-methyl-2-imidazolylmethyl)-*N*-(2'-hydroxy-3',5'-di-*tert*-butylbenzyl)-*N*-(2''-hydroxy-3''-methoxybenzyl)amine, deprotonated form.

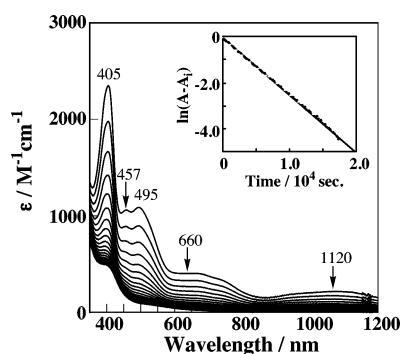


**Figure 6.** Absorption spectral change of **1** after one-electron oxidation by 1 equiv of Ce(IV) at 20°C in CH<sub>3</sub>CN ( $5.0 \times 10^{-4}$  M). Inset: plot of  $\ln[A - A_0]$  at 405 nm vs time.

zero-field splitting parameter calculated from this equation was very small.

**Characterization of Ni(II)–Phenolate Complexes in Solution.** While **1–3** in the solid state were pale blue, yellowish green, and yellowish brown, respectively, their solutions in CH<sub>3</sub>CN gave the same yellowish brown color. The solutions exhibited an absorption peak at 400–450 nm and weak peaks in the range 645–1140 nm ( $\lambda_{\max}$  ( $\epsilon/\text{M}^{-1}\text{cm}^{-1}$ ): **1**, 450 (sh, 900), 646 (45), 998 (50) nm; **2**, 410 (sh, 900), 677 (60), 995 (50) nm; **3**, 400 (sh, 900), 656 (90), 1134 (65) nm). The spectral similarity of the complexes in CH<sub>3</sub>CN may be explained by formation of a similar structure resulting from removal of the water molecule of **1** and dissociation of **2** into the monomeric species. Further, the two broad d–d transition bands at around 650 and 1000 nm are characteristic of 5-coordinate d<sup>8</sup> high-spin Ni(II) structures. These results suggest that **1** and **2** in CH<sub>3</sub>CN have a structure similar to that of **3**. The small differences of the absorption peaks for the complexes are considered to be due to the effect of the donor ability of the nitrogen atoms. However, it is difficult to distinguish between trigonal-bipyramidal and square-pyramidal structures for Ni(II) on the basis of absorption spectra.<sup>18–20</sup> In this connection, 2-(*N*-bis(aminoethyl)-

aminomethyl)phenol was reported to form a mononuclear Ni(II)–phenolate complex in aqueous solution, although X-ray crystal structure analysis showed that the complex has a phenolate-bridged dinuclear structure in the solid state.<sup>21</sup> On the other hand, the absorption band at 400–450 nm ( $\epsilon = 900$ ) is assigned to the phenolate-to-Ni(II) charge transfer (LMCT).<sup>21</sup> Comparison of the  $\lambda_{\max}$  values for **1–3** shows that the transition energy increases with the decrease of the Ni–O(phenolate) bond distance in the order **1** (2.066(3) Å) < **2** (2.017(2) Å) < **3** (1.954(4) Å). This tendency has also been observed for the Cu(II) complexes of the same ligands.<sup>6</sup>

**One-Electron Oxidation.** Addition of an equimolar amount of (NH<sub>4</sub>)<sub>2</sub>Ce(NO<sub>3</sub>)<sub>6</sub>, a one electron oxidant, to **1–3** in CH<sub>3</sub>CN at low temperature caused a color change from pale brown to greenish brown. Oxidized **1** exhibited some new intense absorption bands at 400–500 nm and broad peaks at 660 and 1120 nm (Figure 6). The absorption peaks of oxidized **2** and **3** were very similar to those of oxidized **1** (Table 3). The intense transition band at 394–407 nm may be partly assigned to a  $\pi$ – $\pi^*$  transition of the phenoxy radical, and the spectral features are in good agreement with those of the Ni(II)–phenoxy radical complexes reported.<sup>9,10</sup> The ESR spectra of all the oxidized species at 77 K exhibited an isotropic signal at  $g = 2.23$  (Figure 7). In general,  $S = 1/2$  d<sup>7</sup> low-spin Ni(III) complexes show anisotropic signals at around  $g = 2.2$  and  $g = 2.0$ ,<sup>9,22</sup> but oxidized species of **1–3** are not metal-centered oxidation products, since no

- (18) Lever, A. B. P. *Inorganic Electronic Spectroscopy*, 2nd ed.; Elsevier: New York, 1984.
- (19) Sacconi, L.; Mani, F.; Bencini, A. In *Comprehensive Coordination Chemistry*; Wilkinson, G., Ed.; Pergamon: Oxford, 1987; Vol. 5, Chapter 50.
- (20) (a) Orioli, P. L. *Coord. Chem. Rev.* **1971**, *6*, 285. (b) Morassi, R.; Bertini, I.; Sacconi, L. *Coord. Chem. Rev.* **1973**, *11*, 343.
- (21) Berti, E.; Caneschi, A.; Daiguebonne, C.; Dapporto, P.; Formica, M.; Fusi, V.; Giorgi, L.; Guerri, A.; Micheloni, M.; Paoli, P.; Pontellini, R.; Rossi, P. *Inorg. Chem.* **2003**, *42*, 348.
- (22) Takvoryan, N.; Farmery, K.; Katovic, V.; Lovecchio, F. V.; Gore, E. S.; Anderson, L. B.; Cusch, D. H. *J. Am. Chem. Soc.*, **1974**, *96*, 731.

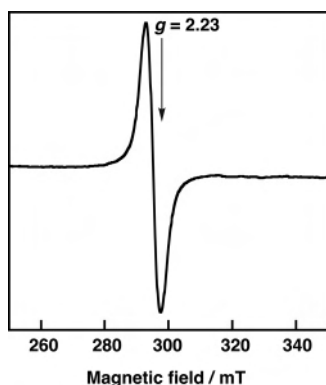


Figure 7. ESR spectrum of one-electron-oxidized **1** in CH<sub>3</sub>CN at 77 K.

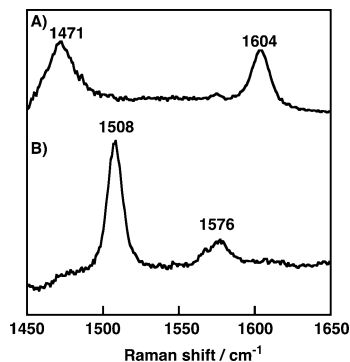


Figure 8. Resonance Raman spectra of (A) **1** and (B) one-electron-oxidized **1**. Measurements were made with 413.1 nm excitation using an Ar<sup>+</sup> laser (power: 50 mW at the sample point) at the sample concentration of 0.5 mM in CH<sub>3</sub>CN.

signals around  $g = 2.0$  were observed. From the spin projection eq 2, an isotropic  $g$  value of 2.23 can be calculated by using a typical  $g_{\text{Ni}}$  value of 2.2 and  $g_{\text{phenoxy}} = 2.0$ :

$$g_{\text{st}=1/2} = \frac{4}{3}g_{\text{Ni}} - \frac{1}{3}g_{\text{radical}} \quad (2)$$

The calculated value of  $g_{\text{st}=1/2}$  of 2.27 is in good agreement with the observations and therefore consistent with the antiferromagnetically coupled system with the  $S = 1$  Ni(II) and  $S = 1/2$  phenoxy radical electrons.<sup>10</sup> These results reveal that one-electron-oxidized **1–3** have an  $S = 1/2$  ground state and that the phenoxy radical is coordinated to Ni(II). However, the constant for the antiferromagnetic coupling,  $-J(H = -JS_1S_2)$ , could not be determined precisely owing to large errors in curve fitting, a rough estimate being  $> 100$  cm<sup>-1</sup>. Regarding the spin state of the complexes, Wieghardt et al. reported that similar octahedral Ni(II) complexes have an  $S = 3/2$  ground state.<sup>10</sup> The present results may be reconciled with their results by considering that complexes **1–3** have a 5-coordinate structure when dissolved in CH<sub>3</sub>CN as described above.

Further evidence for the Ni(II)–phenoxy radical bonding has been provided by comparison of the resonance Raman spectra for a Ni(II)–phenolate complex and its one-electron-oxidized species. The spectra of **1** in the range 1100–1700 cm<sup>-1</sup> obtained before and after Ce(IV) oxidation disclosed that the bands observed for **1** disappeared upon oxidation to give an intense band at 1508 cm<sup>-1</sup> (Figure 8), which corresponds well with the intense 1509 cm<sup>-1</sup> band observed

for one-electron oxidation of [Zn(tbuL)Cl].<sup>6</sup> This band is assigned to the C–O stretching mode ( $\nu_{7a}$ ), which is characteristic of the phenoxy radical species.<sup>23</sup> The observed  $\nu_{7a}$  frequencies of the Ni(II) complexes agree well with those reported for GOase<sup>23</sup> and the Cu(II)- and Zn(II)-coordinated phenoxy radicals of model compounds.<sup>6,24–26</sup>

The difference between complexes **1–3** lies in the stability of their phenoxy radical species. When the green solutions of the oxidized complexes **2** and **3** in CH<sub>3</sub>CN were left to stand at room temperature under anaerobic conditions, they instantly turned colorless, and accordingly the phenoxy radical  $\pi$ – $\pi^*$  transition band at  $\sim 405$  nm disappeared (Figure 6). On the other hand, oxidized **1** was relatively stable at room temperature. Plots of the absorbance at the  $\pi$ – $\pi^*$  band vs time at 20 °C indicated that the intensity decrease was first-order as illustrated for **1** (Figure 6, inset). The decay constants obtained for the radicals of **1–3** and the calculated half-life values are listed in Table 3. The half-life of **1** was 45 min ( $k_{\text{obs}} = 2.48 \times 10^{-4}$  s<sup>-1</sup>) at 20 °C, while the values for **2** and **3** were 26.4 ( $k_{\text{obs}} = 4.38 \times 10^{-4}$  s<sup>-1</sup>) and 5.9 min ( $k_{\text{obs}} = 1.95 \times 10^{-3}$  s<sup>-1</sup>) at –20 °C, respectively, indicating that the stability of the phenoxy radicals from **2** and **3** is comparable with those for the Cu(II) complexes with one or two 2-methylpyridine coordinations.<sup>6</sup> The radical stability can be related with the N-donor ability; the donor nitrogens from the 2-methylpyridyl groups in **2** and **3** are probably weaker than the pyridyl nitrogens of **1** for steric reasons as seen from the structure–radical stability relationship for the corresponding Cu(II) complexes.<sup>6</sup> These results indicate that the stability of the phenoxy radical species is predominantly influenced by the N-donor ability of the ligand stabilizing the Ni(II) state.

The cyclic voltammograms of **1–3** were recorded in CH<sub>3</sub>CN under anaerobic conditions at a scan rate of 50 mV s<sup>-1</sup> in the range 0–1.0 V (Figure 9). For complex **1**, one quasi-reversible redox wave corresponding to the transfer of one electron was observed at 0.56 V vs Ag/AgCl ( $\Delta E = 0.11$  V), and a similar redox wave was also observed for **2** and **3** at 0.49 and 0.56 V, respectively. Electrolysis at 0.85 V of a solution of **1** in CH<sub>3</sub>CN (0.1 M TBAP) at –20 °C showed a transfer of 0.9 electron/mol and a color change to greenish brown. One electron oxidation of **1** yielded an ESR active species with an isotropic signal at  $g = 2.23$ . The properties of the oxidized species were the same irrespective of electrochemical oxidation and chemical oxidation by Ce(IV). On the basis of these results, we assign the above oxidation step to the phenolate/phenoxy radical couple.

We reported earlier that the phenolate/phenoxy radical redox potential for the Cu(II) complex corresponding to **3**

(23) Mukherjee, A.; McGlashen, M. L.; Spiro, T. G. *J. Phys. Chem.* **1995**, *99*, 4912.

(24) Sokolowski, A.; Leutbecher, H.; Weyhermüller, T.; Schnepf, R.; Bothe, E.; Bill, E.; Hildebrandt, P.; Wieghardt, K. *J. Biol. Inorg. Chem.* **1997**, *2*, 444.

(25) Sokolowski, A.; Müller, J.; Weyhermüller, T.; Schnepf, R.; Hildebrandt, P.; Hildebrandt, K.; Bothe, E.; Wieghardt, K. *J. Am. Chem. Soc.* **1997**, *119*, 8889.

(26) Halfen, J. A.; Jazdzewski, B. A.; Mahapatra, S.; Berreau, L. M.; Wilkinson, E. C.; Que, Jr., L.; Tolman, W. B. *J. Am. Chem. Soc.* **1997**, *119*, 8217.

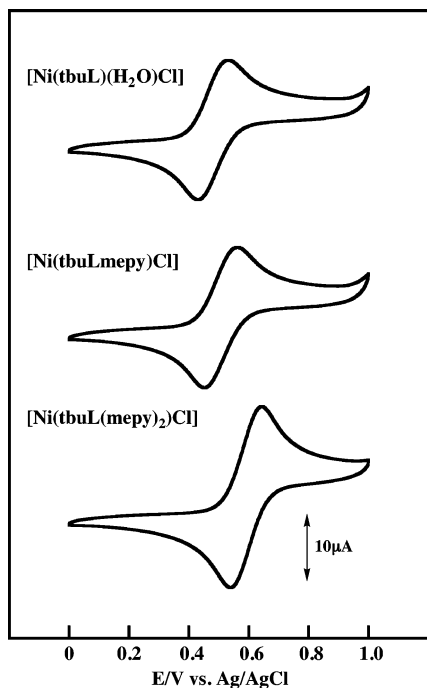


**Figure 9.** Cyclic voltammogram of **1–3** in  $\text{CH}_3\text{CN}$  (1.0 mM) containing 0.1 M  $n\text{-Bu}_4\text{NClO}_4$ . Conditions: working electrode, glassy carbon; counter electrode, Pt wire; reference electrode, Ag/AgCl; scan rate  $50 \text{ mV s}^{-1}$ .

with two *o*-methylpyridine rings was higher than that corresponding to **2** with one *o*-methylpyridine.<sup>6</sup> This may indicate that the equatorial 2-methylpyridine ring is a weaker donor than the unsubstituted pyridine probably for steric reasons. The phenoxyl radical decay constants (Table 3) also show that the radical of the Cu(II) complex corresponding to **2** is more stable than that corresponding to **3** and that the imidazole and unsubstituted pyridine rings equatorially

coordinated to Cu(II) are equally effective in stabilizing the radical.

### Conclusion

We prepared and characterized a series of Ni(II) complexes with  $\text{N}_3\text{O}$ -donor tripodal ligands containing one phenolate moiety with two *tert*-butyl substituents and pyridine rings with and without a methyl group *ortho* to the nitrogen atom. At low temperatures, one electron oxidation of all the Ni(II) complexes yielded the corresponding Ni(II)–phenoxyl radical species, whose decay constants have been determined. The relationship between the structures of the complexes and decay constants indicated that the Ni(II)–phenoxyl radical species is stabilized by pyridine nitrogen donors. The redox potential was lowest for **1** with unsubstituted pyridine rings only and increased in the order  $\mathbf{1} < \mathbf{2} < \mathbf{3}$ , indicating that the radical formation is influenced by the number of the 2-methylpyridine moieties. The observed stability of the radical species for **2** and **3** may be comparable with that of the corresponding Cu(II) complexes previously reported,<sup>6</sup> while the radical species of complex **1** is stable at room temperature. Studies on the metal–phenoxyl binding are in progress in our laboratory.

**Acknowledgment.** This work was supported by a Grant-in-Aid for Scientific Research (No. 16350036) to O.Y. and the “Nanotechnology Support Project” to Kyushu University from the Ministry of Education, Culture, Sports, Science, and Technology of Japan, for which we express our sincere thanks.

**Supporting Information Available:** Crystallographic data (excluding structure factors) for complexes **1–3** in CIF format. This material is available free of charge via the Internet at <http://pubs.acs.org>.

IC049040K